Structure, Vol. 9, 1043–1050, November, 2001, ©2001 Elsevier Science Ltd. All rights reserved. PII S0969-2126(01)00674-8

The Ras-Byr2RBD Complex: Structural Basis for Ras Effector Recognition in Yeast

Klaus Scheffzek,[1,2,3] Petra Grünewald,[1] Sabine Wohlgemuth,[1] Wolfgang Kabsch,[2] Hua Tu,[4] Mike Wigler, [4] Alfred Wittinghofer,[1] and Christian Herrmann[1,5]

[1] Max-Planck-Institut für molekulare Physiologie
Abt. Strukturelle Biologie
Otto-Hahn-Str. 11
44227 Dortmund
Germany

[2] Max-Planck-Institut für medizinische Forschung
Abt. Biophysik
Jahnstr. 29
69120 Heidelberg
Germany

[3] European Molecular Biology Laboratory
Structural and Computational Biology Programme
Meyerhofstr. 1
69117 Heidelberg
Germany

[4] Cold Spring Harbor Laboratory
Cold Spring Harbor, New York 11724

Summary

Background: The small GTP binding protein Ras has important roles in cellular growth and differentiation. Mutant Ras is permanently active and contributes to cancer development. In its activated form, Ras interacts with effector proteins, frequently initiating a kinase cascade. In the lower eukaryotic *Schizosaccharomyces pombe*, Byr2 kinase represents a Ras target that in terms of signal-transduction hierarchy can be considered a homolog of mammalian Raf-kinase. The activation mechanism of protein kinases by Ras is not understood, and there is no detailed structural information about Ras binding domains (RBDs) in nonmammalian organisms.

Results: The crystal structure of the Ras-Byr2RBD complex at 3 Å resolution shows a complex architecture similar to that observed in mammalian homologous systems, with an interprotein β sheet stabilized by predominantly polar interactions between the interacting components. The C-terminal half of the Ras switch I region contains most of the contact anchors, while on the Byr2 side, a number of residues from topologically distinct regions are involved in complex stabilization. A C-terminal helical segment, which is not present in the known mammalian homologous systems and which is part of the auto-inhibitory region, has an additional binding site outside the switch I region.

Conclusions: The structure of the Ras-Byr2 complex confirms the Ras binding module as a communication element mediating Ras-effector interactions; the Ras-Byr2 complex is also conserved in a lower eukaryotic system like yeast, which is in contrast to other small GTPase families. The extra helical segment might be involved in kinase activation.

[5] Correspondence: christian.herrmann@mpi-dortmund.mpg.de

Introduction

Ras proteins are key elements in intracellular signaling and are involved in a variety of vital processes such as DNA transcription, growth control, and differentiation. They function like molecular switches cycling between GTP bound "on" and GDP bound "off" states [1, 2]. The biological activity of Ras is controlled by at least two kinds of regulators: guanine nucleotide exchange factors (GEFs) that increase the nucleotide dissociation rate to facilitate binding of cellular abundant GTP and GTPase activating proteins (GAPs) that accelerate the rate of GTP hydrolysis to return Ras to the inactive GDP bound form [3, 4]. Two regions, termed switch I and switch II, have been identified as major segments that define the conformational differences between active and inactive Ras [5]. When bound to GTP, Ras is able to interact with effector proteins to trigger a variety of cellular responses. At least three effectors have been identified in mammalian cells: Raf kinase, PI(3) kinase, and RalGDS [6]. A common feature of these is the Ras binding domain that, despite absence of sequence similarity, shares the ubiquitin fold as a common structural motif [7–12]. Structural work has so far characterized Ras effector binding as the formation of an interprotein β sheet that is stabilized mainly by polar interactions between the switch I region of Ras and the N-terminal β strands of RBD including a midhelix [13–17].

Byr2 is a Ser/Thr-specific protein kinase acting as mediator of signals for sexual differentiation in *Schizosaccharomyces pombe* by initiating a MAPK module, which is a highly conserved element in eukaryotes [18–20]. It is a homolog of mammalian MEKK, and both are at the same hierarchic level as Raf in the respective MAPK module, i.e., they are activated through interaction with Ras. It was demonstrated earlier that the Ras binding domain (RBD) of Byr2 is necessary and sufficient for the protein to be translocated by Ras to the plasma membrane [21]. The RBD of Byr2 is located in the regulatory half of the protein at the amino terminus [22]. This RBD was isolated as a protein fragment comprising residues 65–180 or an N-terminally shorter version (residues 71–180). As a first example of a Ras-effector complex from nonmammalian organisms, we have characterized the interaction between Ras and Byr2RBD by biochemical methods and have determined the three-dimensional structure of the complex of the two proteins by X-ray crystallography.

Key words: Byr2-kinase; mutational analysis; *Schizosaccharomyces pombe*; Ras signaling; GTP binding protein, cancer; GTPase; X-ray crystallography

Table 1. Summary of Crystallographic Analysis

Data Collection	
Resolution (Å)	3.0
Highest shell	3.1–3.0
Number of observations	109,981 (2,634)
Number of unique reflections	8,526 (788)
Completeness (%)	99.7 (100)
R_{symm} (%)[a]	13.9 (30.5)
I/σ	18.6 (4.1)
Refinement	
Resolution range (Å)	25–3
Number of reflections	8526
R_{work} (%)[b]	23.6
R_{free} (%)[c]	31.2
Rmsd bonds (Å)	0.008
Rmsd angles (deg)	1.375

Numbers in parentheses refer to highest resolution shell.

[a] $R_{symm} = \sum_h \sum_i | I_{hi} - I_h | / \sum_{hi} I_{hi}$, where I_{hi} is the scaled intensity of the i^{th} symmetry related observation of reflection h and I_h is the mean value.

[b] $R_{work} = \sum_h | F_{oh} - F_{ch} | / \sum_h F_{oh}$, where F_{oh} and F_{ch} are the observed and calculated structure factor amplitudes for reflection h.

[c] R factor calculated for 10% randomly chosen reflections not included in the refinement.

Results and Discussion

Structure of Byr2RBD

The complex between Byr2RBD (71–180) and GppNHp bound *H*-Ras (1–166) was purified and crystallized, and the structure was determined at 3 Å resolution, as described in the Experimental Procedures. The current model covers the full H-Ras molecule and Byr2 residues 71–165; a middle segment of residues 127–139 and the end residues 166–180 were ill defined in the electron density. Although a shorter construct of Byr2RBD (residues 71–171) in complex with Ras has improved crystallization properties, the resolution remains in the same range as it does for the longer version. A summary of the crystallographic data analysis is given in Table 1.

The structure of the Ras-Byr2RBD complex (Figure 1a) reveals Byr2RBD to have essentially the ubiquitin fold as observed for the RBDs of Raf-kinase [8, 9], RalGDS [7, 12], Rlf [10], Rgl [23], and PI(3) kinase [11], consistent with the recent NMR assignment [24]. A mixed five-stranded β sheet is flanked by at least two helical segments (see below), one of which seems to be flexible in our crystals. An additional helix (α3) was found at the C-terminal end of Byr2RBD with no counterpart in either of the RBDs known so far. A structure-based sequence alignment is shown in Figure 1b. As mentioned above, the segment covering residues 127–139 is not ordered in the crystal, but electron density suggests some helical contents. Comparison with the NMR model (see Gronwald et al. [74] in this issue) confirms the basic fold, particularly in defining the second α helix (α2) in solution.

The Complex Interface

The complex shows a similar protein-protein interaction pattern as that seen in previously solved Ras effector complex structures with an interprotein β sheet as the most apparent feature (Figure 1a). It buries about 1200 Å^2 of solvent-accessible surface area in its interface, similar to the other known Ras complexes with Raf [13, 14], RalGDS [15, 16], and PI(3) kinase [17]. The switch regions I and II of Ras, which have been defined as protein segments that change their conformation upon transition between GTP and GDP bound forms [5], are in the canonical GTP bound conformation [25]. In particular, Tyr32 from switch I is closing upon the phosphate binding region and interacts with the γ-phosphate. The situation is consistent with the guanine nucleotide dissociation inhibitory (GDI) effect resulting from interaction of RBDs with Ras, as observed earlier [26]. Since mammalian Ras and Ras1 from *S. pombe* are highly homologous and the interacting residues are totally conserved, we

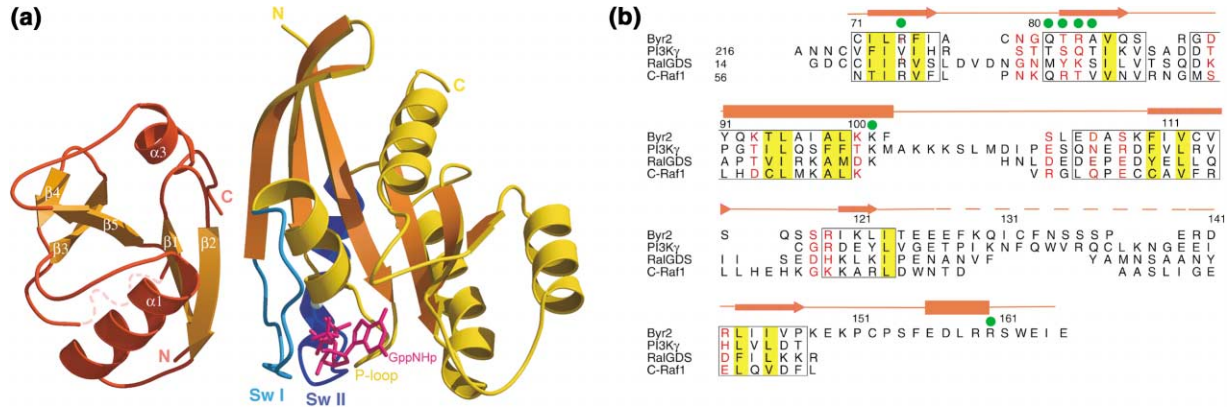

Figure 1. The Ras-Byr2RBD Complex

(a) Ribbon representation showing Byr2RBD on the left and Ras on the right. Switch I is shown in light blue, switch II is in dark blue, and the nucleotide is in pink. The presumed helical segment in the middle of the RBD is indicated as a dashed wavy line.

(b) Structure-based sequence alignment of the RBDs from Raf [13], PI3-kinase [17], RalGDS [7], and Byr2 (this work), done with the program STAMP [72]. Assignment of secondary structure elements according to the program DSSP [73] is included for Byr2RBD; dashed lines indicate disordered regions. Structurally related regions are boxed and residues conserved as hydrophobic or polar amino acids are in yellow and red, respectively. Residues involved in the interaction with Ras are marked with green dots.

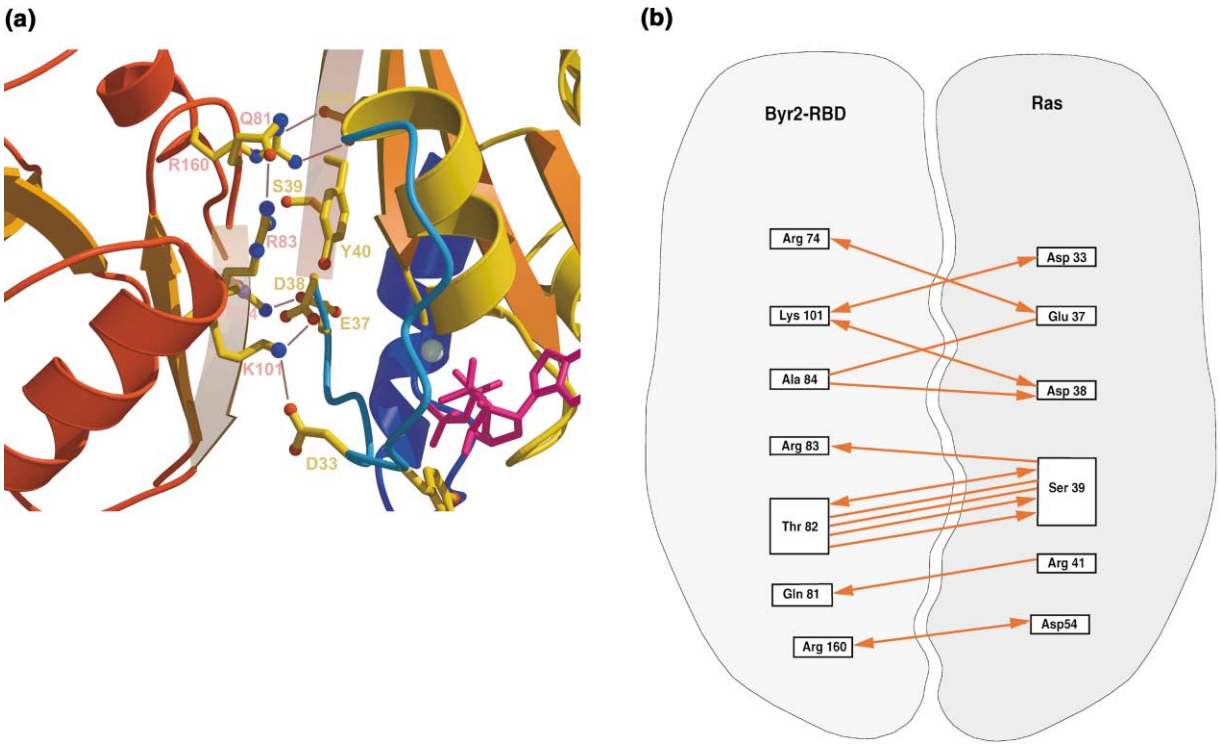

Figure 2. View of the Complex Interface

(a) Close-up view of the complex interface with selected side chains involved in interprotein interactions included.

(b) Cartoon of the complex interface indicating favorable interactions (red lines) inferred from the structural model. Arrow heads indicate side chain, and straight ends indicate main chain contribution to the respective interactions.

can assume that the present structure is a very close homolog of the real *S. pombe* complex.

As far as the definition of interactions is possible given the limited resolution, polar contacts seem to play a major role in the complex stabilization (Figure 2a). A schematic view of the interface is given in Figure 2b. As observed in mammalian Ras effector complexes, similar residues on the Ras side are involved in complex formation. These polar interactions involve residues almost exclusively from switch I, particularly Asp33, Glu37, Asp38, Ser39, and Arg41; these same residues are also involved in the interaction with the Raf kinase [13, 14] and PI(3)kinase [17], whereas the RalGDS complex does not use Ser39 or Arg41 [15, 16]. As in the Raf kinase and RalGDS complex, no residues from switch II are employed for the interaction, in contrast with the complex with PI(3)kinase where Ras also uses residues from switch II, presumably for allosterically regulating the kinase [17]. Strikingly, Asp30 and Glu31, residues that determine target specificities of Rap and Ras toward the RBDs of Raf and RalGDS, respectively [14, 27], do not show contacts with Byr2RBD (see below).

On the Byr2 side, most of the residues participating in intermolecular interactions are located in strand β2 (Figures 1b and 2a), representing the edge of the protein that is directed toward Ras. They are primarily polar in character, and they mainly contact amino acids in the stretch from residue 38 to 41 of Ras. The guanidinium group of $Arg83_{Byr}$ is in close proximity of the effector loop main chain region, allowing a polar contact with the carbonyl oxygen of Ser39. $Arg74_{Byr}$ in strand β1 forms a salt bridge with the carboxylate group of Glu37. The side chain of $Lys101_{Byr}$ at the C-terminal end of helix α1 is in an orientation where a salt bridge may be formed with Asp33 or Asp38. This situation is reminiscent of the Ras-RasGAP complex where a conserved lysine (Lys949 of p120GAP) interacts with these two residues in a similar geometry [28]. The Byr2 mutant K101E was reported to disrupt interaction between Ras and Byr2 [22]. Finally, a contact conceivable from the C-terminal α helix of Byr2RBD to the G domain core of Ras.

Mutational Analysis of the Interface

In order to analyze the contribution of individual residues participating in intermolecular interactions, we have carried out site-directed mutagenesis studies. The interaction between Ras and Byr2RBD (65–180) was quantified by the GDI method as described earlier for other Ras effectors like the RBDs of Raf, RalGDS, and AF6 [27, 29]. On the Ras side, we selected for substitution those residues that comprise the classical effector region (residues 32–40) as well as residues flanking this region on both sides. We prepared a number of mutants that have been used as partial loss-of-function in mammalian cell culture studies and/or have been studied extensively for interaction with different effectors. These mutations are supposed to weaken the interaction with some effectors and leave it intact with others [30–38]. On the Byr2 side, residues were selected on the basis of the observed contacts in the present structure of the Ras-

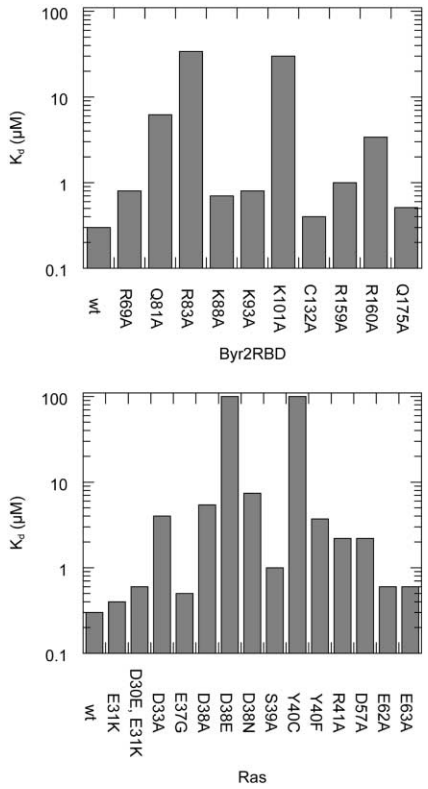

Figure 3. Mutational Analysis

K_d values (μM) for the Ras-Byr2 interaction as determined by the GDI assay at 37°C. The experimental error on the K_d values is 20%. The values of 100 μM represent the lower estimates for each of the two mutants.

Byr2RBD complex. The results for the Ras and the Byr2 mutants are represented in Figure 3. No difference in Ras binding affinity was observed between the 65–171 and the 65–180 constructs (data not shown). The results will be discussed in the context of the structural findings.

The effects of Ras mutations may be grouped into four categories. First, in the classical effector region, three residues play an important role for the interaction with Byr2, i.e., Asp33, Asp38, and Tyr40. When Asp33 and Asp38 are mutated to Ala, a greater than 10-fold increase of the K_d value is observed for each. The same is true for Y40F, which is somewhat surprising since the hydroxyl group is not likely to form polar contacts within the interface. In the case of Asp38, it is interesting to note that on the one hand a longer side chain is not tolerated, since D38E has an even much more pronounced effect on the binding affinity indicating repulsive effects; and on the other hand, the negative charge seems to play a major role, since the D38N and D38A mutants show a somewhat smaller effect with 25- and 18-fold reduction, respectively. The latter finding is quantitatively different from the 10-fold difference for D38N and D38A found by Ohnishi et al. [39]. However, considering that they used wild-type and mutant Ras peptides instead of the intact RBD, the results are remarkably consistent. The Asp38→Glu mutation has been shown to have a major effect on Ras effector and Ras-RasGAP interactions, underscoring the importance of Asp38 for the interaction with effectors and regulators [6, 40]. As discussed above, Asp33 and Asp38 are both potential salt-bridging partners for $Lys101_{Byr}$, located on the C-terminal end of helix α1 in the RBD. Irrespective of the possible number of interactions (arrows in Figure 2b), the side chain of Ser39 seems to provide no contribution for Byr2 binding, since the alanine mutation increases the K_d value only 3-fold. The contribution of the main chain contacts emanating from Ser39 (Figure 2b) are not accessible by mutational analysis. Thr35 is a residue totally conserved in all GTP binding proteins and is involved in the switch mechanism by virtue of being bound to the γ-phosphate [41]. The T35S mutant, which has been used as a partial loss-of-function mutation specific for the Ras pathway, is nevertheless compromised in its ability to interact with all effectors, even though it is not involved in any direct interaction. Similarly, in the Ras-Byr2RBD complex, Thr35 is not in direct contact, but the T35S mutation increases the K_d 12-fold, most likely due to a change in the dynamic properties of Ras [42].

The second category is residues flanking the effector region. As mentioned above, determinants of Ras/Rap effector specificity toward Raf and RalGDS turned out not to be involved in the binding to Byr2RBD. Mutation of Ras residues Asp30 and Glu31 to the corresponding residues in Rap proteins, Glu and Lys, results in only a 2-fold increase of the K_d value. This is consistent with the observation that these residues are not contributing to the complex interface in our structure. In contrast, Arg 41, which is highly conserved within the Ras subfamily, has a modest contribution to the interaction with Byr2, with a 7-fold reduction of affinity observed for the R41A mutant.

The third category is partial loss of function mutants. The E37G mutation was one of the first partial loss of function mutants discovered, which established the concept that Ras uses multiple pathways for cell transformation. It was found in a two-hybrid screen as a mutant that fails to interact with Raf but is unimpaired for Byr2 binding [30]. Since the mutation has only a minor effect on the interaction, the salt bridge with $Arg74_{Byr}$ is probably less important. Other commonly employed mutations of that category include Y40C and D38E, which show rather large effects on binding. Both heavily interfere with the Byr2RBD interaction to an extent that their affinity cannot be measured with the GDI technique. Although Asp38 is also involved in the Ras-Raf interaction, the D38E mutation has only a small effect on that interaction. This highlights the notion that the analysis of a protein-protein interface by a three-dimensional structure does not per se indicate the importance of individual residues for the interaction and/or allow us to predict a priori the effect of a particular mutation. While the effect of Cys in position 40 can apparently not be rationalized from our structural model, the possible contact between Asp38 and $Lys101_{Byr}$ makes a modest contribution to the binding affinity (Figure 2a).

The fourth category is mutants in the switch II region. The glutamate residues at positions 62 and 63 do not participate in the Ras-Byr2RBD interaction, as indicated by only a 2-fold change in affinity for the Ala mutants. This is not unexpected, as these residues are solvent exposed and are not involved in the interaction with the Byr2RBD. The same was observed for the interaction

between Ras and RalGDS [16], although crystal contacts with a symmetry-related molecule via these residues had been suggested to contribute to the interaction [7]. The decreased binding affinity of the D57A mutant can be explained by altered Mg^{2+} coordination, which has an effect on nucleotide binding and thereby on Byr2 interaction.

On the Byr2RBD side, there are two residues contributing strongly to the interaction; their mutation to Ala leads to a 100-fold decrease in affinity. One of these is $Lys101_{Byr}$ which was discovered earlier in a screen for Ras/Byr2 disruptive mutants [22] and is close enough to both Asp33 and Asp38 for salt bridges. A similar crucial salt bridge is described for Arg89 from c-Raf, which is located in the center of the Ras-Raf interface [13, 14] and has also been found in a genetic screen of the *Drosophila* sevenless pathway [43]. A similar large contribution to the binding energy is due to $Arg83_{Byr}$, whereas mutation of $Gln81_{Byr}$ reduces the affinity a moderate 20-fold. Given the mutual stabilization of $Arg83_{Byr}$ and $Gln81_{Byr}$ (Figure 2), the observed effects on binding affinity may be strongly interdependent. Interestingly, $Arg160_{Byr}$ from the C-terminal helix moderately contributes to binding and is in the structure in proximity to Asp54 of Ras. Overall, the interaction between Ras and Byr2 is dominated by charge-charge interactions, where Byr2RBD is primarily positively charged. This was also observed for Raf, RalGDS, and PI(3)K [14–17], and it appears to be a common feature for Ras effectors to be a complement to the negative surface potential of Ras in the effector region.

Concluding Remarks

Based on the primary sequence, it seems difficult to predict Ras effectors or at least their RBDs. Some of the RBDs or Ras-associating (RA) domains predicted do not show any interaction with Ras, e.g., the unconventional myosin and Rho-GAP myr5 [44, 45]. On the other hand, there are a number of RBDs that do not show up in the database search like the RBDs of Raf and Byr2. Nevertheless, Ras-effector interaction has been demonstrated to show a high level of structural conservation. This reiterates earlier observations that different effectors of Ras, now including the effector Byr2 of Ras1 in the yeast *S. pombe*, have no recognizable sequence conservation but yet show the same three-dimensional structure and the very stable ubiquitin superfold [46] and also react with Ras (Ras1) in the same basic interaction pattern by forming an interprotein β sheet. During complex formation, there is no appreciable conformational change involving the effector [7, 8, 11–17]. This is in contrast to members of the Rho family, where the effectors of Rac and Cdc42 contain a region with conserved sequence homology, the CRIB or GBD region [47, 48], which does not form a stable fold [49–53]. Here, complex formation with the GTP binding protein involves a large conformational change.

Biological Implications

A number of kinases are effectors of GTP binding proteins of the Rho and Ras subfamily in that the binding is dependent on the triphosphate conformation [6]. Binding, in turn, induces activation of kinases, as demonstrated in vitro and in vivo for PAK [54, 55] and Rho kinases [56, 57]. Activation, in addition to translocation, is also discussed for the interaction between Ras and Raf [58, 59], although structural models for such a mechanism do not exist. For PAK it has been shown that the N-terminal regulatory domain binds directly to and thereby inhibits the catalytic domain [60, 61], and structural studies on a complex between the regulatory and the catalytic domain on one side [62] and on the complex between Cdc42-GTP and a regulatory fragment on the other side [51, 63] have suggested how the binding of the G protein induces a large conformational change which relieves the inhibition of the catalytic domain.

A similar interaction has been demonstrated for Byr2, where a detailed mapping of the protein has identified an RBD, residues 71–180, and a domain that binds the catalytic domain (CBD), residues 151–260 [22]. These authors have also shown that these two domains overlap considerably. In the present structure we have used an RBD fragment that contains part of the CBD. Indeed, the structure shows that the present construct contains an extra helix (α3) that is not present in either RafRBD or RalGDS-RBD. This helix is close to Ras and actually is involved in the interface by forming an interaction between $Arg160_{Byr}$ and Asp54 in β strand 3 of Ras; there are even more potentially interacting pairs of residues in this area of the interface. The 10-fold increase of the K_d value after mutation of $Arg160_{Byr}$ supports the observation that the additional helix α3 contributes to the interaction with Ras. It could thus easily be envisioned that the binding of Ras•GTP to the RBD induces a structural change in the CBD that releases the inhibitory interaction with the catalytic domain and thus leads to activation of the kinase activity of Byr2. Obviously this model has to be verified by further structural studies on larger fragments of Byr2, which include the complete CBD and the kinase domain.

Is the envisioned activation mechanism unique for nonmammalian Ras effectors or would there be implications for other effector interaction? Raf kinase contains, in addition to the RBD, a cysteine-rich domain (CRD). This CRD is directly C-terminal to the RBD, and it has been shown that while the interaction of Ras with RBD is necessary for the translocation of Raf to the plasma membrane, the interaction with CRD is believed to be crucial for the activation of the kinase (see [64]). It has further been shown that residues near switch II or near residue 45 are involved in the interaction with the CRD [65, 66]. In the analogy to Byr2, one could imagine that Ras binds to Raf in a bipartite interaction mode similar to what we find for Ras-Byr2, with the second site being involved in activation. Confirmation for such a scenario comes from the structure of the Ras-PI(3)Kγ complex, where Ras uses the conventional RBD for a canonical interprotein β sheet interaction. In addition, it interacts with the catalytic part of the kinase via the switch II region, and it is believed that this interaction induces the well-documented activation of the kinase activity [17].

Experimental Procedures

Protein Purification and Characterization

H-Ras (1–166) was synthesized in *Escherichia coli* and purified from the cleared cell lysate by ion exchange chromatography followed by

size exclusion chromatography, as reported earlier [67]. Exchange of the bound GDP for the nonhydrolyzable GTP analog GppNHp or the fluorescent mant-analog thereof is described in [27]. The Ras binding domain of Byr2 kinase (Byr2RBD) was cloned in a pGEX-2T plasmid leading to the synthesis of the glutathione S-transferase fusion protein in *Escherichia coli* strain BL21. After purification, according to standard protocols and cleavage of the fusion protein with thrombin, the Byr2RBD fragment was subjected to size-exclusion chromatography (Superdex-75, Pharmacia). A dimer and a monomer fraction of similar sizes were eluted from the column; both were stable as such. Also for Byr2RBD in complex with Ras, dimer and monomer fractions were collected from the size exclusion column. The proteins were concentrated to 20–25 mg/ml by using centrifugal concentrators (VivaScience) and were stored at −80°C after snap freezing in liquid nitrogen. The Byr2RBD fragments used in this study comprise amino acids 65–171 and 65–180 or 71–180, respectively. Specific mutations were introduced by applying standard PCR mutagenesis protocols. All proteins prepared were more than 90% pure as judged from Coomassie-stained polyacrylamid gels.

The affinities between Byr2 mutants and Ras and mutants thereof were quantified by taking advantage of the GDI (guanine nucleotide dissociation inhibitor) effect. Like other effectors, Byr2 binding to Ras leads to decreased dissociation rates of the nucleotide. This process can easily be followed by using mant-GppNHp. The kinetics of nucleotide dissociation are recorded by a spectrofluorimeter (Fluoromax, Spex) exciting the fluorescence at 360 nm and monitoring at 450 nm. Ras (at 50 nM) in complex with mant-GppNHp is incubated with different concentrations of Byr2RBD, and the mant-GppNHp displacement is started by the addition of 100 μM GppNHp. The rate constants are measured in dependence of the Byr2 concentration, allowing the calculation of the equilibrium dissociation constant K_d of the Ras-Byr2RBD complex as described [27]. The buffer used for these experiments contained 50 mM Tris HCl at pH 7.4, 5 mM $MgCl_2$, 100 mM NaCl, and 2 mM DTE.

Crystallization

While the fraction corresponding to dimeric Ras-Byr2RBD (71–180) yielded only pseudocrystalline aggregates, single crystals could be grown from the monomeric species under a variety of conditions, including using ammonium sulfate and sodium formate as precipitants. Diffraction-quality crystals were grown at room temperature by using the hanging-drop method. Equal volumes (2–5 μl) of protein (20–25 mg/ml) and precipitant solution (composed of 20%–25% polyethylene glycole (PEG) 3350 in 100 mM Tris HCl [pH 8] with 0.2–0.4 M $LiSO_4$) were mixed on a cover slide and suspended above a reservoir containing 0.4 ml of precipitant solution. Crystals appeared within hours or days depending on the quality of the protein preparation and on conditions.

They grew to an average size of 100 × 100 × 400 μm^3 and diffracted to about 3 Å with a rotating anode or synchrotron radiation. Attempts to improve diffraction quality, e.g., by using other Ras isoforms such as K-Ras or N-Ras remained unsuccessful.

Data Collection, Structure Determination, and Refinement

For data collection, crystals were mounted in glass/quartz capillaries and cooled to ~4°C. Data were collected with the rotation method (wavelength CuKα, 1.5419 Å; crtstal detector distance 12 cm; oscillation range 0.0833°), by using a rotating anode generator (Elliott, GX18) as the X-ray source and a Siemens/Nicolett multiwire area detector for data recording. Data from four crystals were processed and scaled with the program XDS [68], and the space group was determined to be rhombohedral R32 with unit cell dimensions a = b = 139 Å, c = 112.8 Å. Structure determination was done with the molecular replacement method by using the refined coordinates of Ras:GppNHp [25] without ligands as search model in rotation and translation search calculations carried out with the program AMoRe [69] (CCP4, [77]). We obtained an optimum set of rotation angles 9°/60°/31°. Translation by fractional coordinates 0.51/0.31/0 resulted in a position that was compatible with lattice packing and could be refined to an R factor of 45%. An initial electron density map calculated with the phases of the Ras component showed clear density for the nucleotide bound to the protein and for features of the RBD. In alternate rounds of interactive model building (program O, [70]) and refinement (program CNS, [71]), with the RafRBD model [13] as a guide, the Byr2RBD component was completed to residues 71–165, with the exception of the presumably helical segment of residues 127–139, which showed only poor electron density. The NMR model (see Gronwald et al. [74] in the accompanying paper) confirms the helical contents of the segment (see the structure description). A number of side chains did not show reasonable electron density and were therefore modeled stereochemically. These include Arg98, Gln92, Lys93, Glu105, Lys109, Gln116, Ser117/118, Arg119, Glu126, Arg140, and Phe155 in Byr2RBD. Structure visualization was done with the programs MOLSCRIPT [75] and Raster 3D [76].

Acknowledgments

We thank Rob Russell for help with STAMP, and K.S. is grateful to K. Holmes for continuous support. For financial support C.H. is grateful to EC (QLK3-CT-1999-00875), P.G. to Deutsche Forschungsgemeinschaft (SFB394), and K.S. to the Peter and Traudl Engelhorn Stiftung.

Received: August 17, 2001
Accepted: October 17, 2001

References

1. Bourne, H.R., Sanders, D.A., and McCormick, F. (1990). The GTPase superfamily: a conserved switch for diverse cell functions. Nature *348*, 125–132.
2. Bourne, H.R., Sanders, D.A., and McCormick, F. (1991). The GTPase superfamily: conserved structure and molecular mechanism. Nature *349*, 117–127.
3. Boguski, M.S., and McCormick, F. (1993). Proteins regulating Ras and its relatives. Nature *366*, 643–654.
4. McCormick, F. (1995). Ras-related proteins in signal transduction and growth control. Mol. Reprod. Dev. *42*, 500–506.
5. Milburn, M.V., et al., and Kim, S.-H. (1990). Molecular switch for signal transduction: structural differences between active and inactive forms of protooncogenic *ras* proteins. Science *247*, 939–945.
6. McCormick, F., and Wittinghofer, A. (1996). Interactions between Ras proteins and their effectors. Curr. Opin. Biotechnol. *7*, 449–456.
7. Huang, L., Weng, X.W., Hofer, F., Martin, G.S., and Kim, S.H. (1997). Three-dimensional structure of the Ras-interacting domain of RalGDS. Nat. Struct. Biol. *4*, 609–615.
8. Emerson, S.D., et al., and Fry, D.C. (1995). Solution structure of the Ras-binding domain of c-Raf-1 and identification of its Ras interaction surface. Biochemistry *34*, 6911–6918.
9. Emerson, S.D., Waugh, D.S., Scheffler, J.E., Tsao, K.L., Prinzo, K.M., and Fry, D.C. (1994). Chemical shift assignments and folding topology of the Ras-binding domain of human Raf-1 as determined by heteronuclear three-dimensional NMR spectroscopy. Biochemistry *33*, 7745–7752.
10. Esser, D., Bauer, B., Wolthuis, R.M., Wittinghofer, A., Cool, R.H., and Bayer, P. (1998). Structure determination of the Ras-binding domain of the Ral-specific guanine nucleotide exchange factor Rlf. Biochemistry *37*, 13453–13462.
11. Walker, E.H., Perisic, O., Ried, C., Stephens, L., and Williams, R.L. (1999). Structural insights into phosphoinositide 3-kinase catalysis and signalling. Nature *402*, 313–320.
12. Geyer, M., Herrmann, C., Wohlgemuth, S., Wittinghofer, A., and Kalbitzer, H.R. (1997). Structure of the Ras-binding domain of RalGEF and implications for Ras binding and signalling. Nat. Struct. Biol. *4*, 694–699.
13. Nassar, N., Horn, G., Herrmann, C., Scherer, A., McCormick, F., and Wittinghofer, A. (1995). The 2.2 Å crystal structure of the Ras-binding domain of the serine/threonine kinase c-Raf1 in complex with Rap1A and a GTP analogue. Nature *375*, 554–560.
14. Nassar, N., Horn, G., Herrmann, C., Block, C., Janknecht, R., and Wittinghofer, A. (1996). Ras/Rap effector specificity determined by charge reversal. Nat. Struct. Biol. *3*, 723–729.
15. Huang, L., Hofer, F., Martin, G.S., and Kim, S.H. (1998). Structural

basis for the interaction of Ras with RalGDS. Nat. Struct. Biol. *5*, 422–426.
16. Vetter, I.R., et al., and Wittinghofer, A. (1999). Structural and biochemical analysis of Ras-effector signaling via RalGDS. FEBS Lett. *451*, 175–180.
17. Pacold, M.E., et al., and Williams, R.L. (2000). Crystal structure and functional analysis of Ras binding to its effector phosphoinositide 3-kinase gamma. Cell *103*, 931–943.
18. Wang, Y., Xu, H.-P., Riggs, M., Rodgers, L., and Wigler, M. (1991). byr2, a Schizosaccharomyces pombe gene encoding a protein kinase capable of partial suppression of the ras1 mutant phenotype. Mol. Cell. Biol. *11*, 3554–3563.
19. Van Aelst, L., Barr, M., Marcus, S., Polverino, A., and Wigler, M. (1993). Complex formation between RAS and RAF and other protein kinases. Proc. Natl. Acad. Sci. USA *90*, 6213–6217.
20. Masuda, T., Kariya, K., Shinkai, M., Okada, T., and Kataoka, T. (1995). Protein-kinase byr2 is a target of ras1 in the fission yeast schizosaccharomyces-pombe. J. Biol. Chem. *270*, 1979–1982.
21. Engh, R.A., et al., and von der Saal, W. (1996). Enzyme flexibility, solvent and 'weak' interactions characterize thrombin-ligand interactions: implications for drug design. Structure *4*, 1353–1362.
22. Tu, H., Barr, M., Dong, D.L., and Wigler, M. (1997). Multiple regulatory domains on the Byr2 protein kinase. Mol. Cell. Biol. *17*, 5876–5887.
23. Kigawa, T., Endo, M., Ito, Y., Shirouzu, M., Kikuchi, A., and Yokoyama, S. (1998). Solution structure of the Ras-binding domain of RGL. FEBS Lett. *441*, 413–418.
24. Huber, F., et al., and Kalbitzer, H.R. (2000). Letter to the editor: sequential NMR assignment of the RAS-binding domain of Byr2. J. Biomol. NMR *16*, 355–356.
25. Pai, E.F., Krengel, U., Petsko, G.A., Goody, R.S., Kabsch, W., and Wittinghofer, A. (1990). Refined crystal structure of the triphosphate conformation of H-*ras* p21 at 1.35 Å resolution: implications for the mechanism of GTP hydrolysis. EMBO J. *9*, 2351–2359.
26. Herrmann, C., Martin, G.A., and Wittinghofer, A. (1995). Quantitative analysis of the complex between p21ras and the Ras-binding domain of the human Raf-1 protein kinase. J. Biol. Chem. *270*, 2901–2905.
27. Herrmann, C., Horn, G., Spaargaren, M., and Wittinghofer, A. (1996). Differential interaction of the ras family GTP-binding proteins H-Ras, Rap1A, and R-Ras with the putative effector molecules Raf kinase and Ral-guanine nucleotide exchange factor. J. Biol. Chem. *271*, 6794–6800.
28. Scheffzek, K., et al., and Wittinghofer, A. (1997). The Ras-RasGAP complex: structural basis for GTPase activation and its loss in oncogenic Ras mutants. Science *277*, 333–338.
29. Linnemann, T., et al., and Herrmann, C. (1999). Thermodynamic and kinetic characterization of the interaction between the Ras binding domain of AF6 and members of the Ras subfamily. J. Biol. Chem. *274*, 13556–13562.
30. White, M.A., et al., and Wigler, M. (1995). Multiple ras functions can contribute to mammalian-cell transformation. Cell *80*, 533–541.
31. White, M.A., et al., and Barsagi, D. (1996). A role for the ral guanine nucleotide dissociation stimulator in mediating ras-induced transformation. Stimulation of membrane ruffling and map kinase activation by distinct effectors of Ras. J. Biol. Chem. *271*, 16439–16442.
32. Akasaka, K., et al., and Kataoka, T. (1996). Differential structural requirements for interaction of ras protein with its distinct downstream effectors. J. Biol. Chem. *271*, 5353–5360.
33. Joneson, T., White, M.A., Wigler, M.H., and Barsagi, D. (1996). Stimulation of membrane ruffling and map kinase activation by distinct effectors of ras. Science *271*, 810–812.
34. Rodriguez-Viciana, P., Warne, P.H., van Haesebroeck, B., Waterfield, M.D., and Downward, J. (1996). Activation of phosphoinositide 3-kinase by interaction with Ras and by point mutation. EMBO J. *15*, 2442–2451.
35. Rodriguez-Viciana, P., et al., and Downward, J. (1997). Role of phosphoinositide 3-OH kinase in cell transformation and control of the actin cytoskeleton by Ras. Cell *89*, 457–467.
36. Khosravifar, R., et al., and Der, C.J. (1996). Oncogenic Ras activation of Raf/mitogen-activated protein kinase-independent pathways is sufficient to cause tumorigenic transformation. Mol. Cell. Biol. *16*, 3923–3933.
37. Wolthuis, R.M.F., de Ruiter, N.D., Cool, R.H., and Bos, J.L. (1997). Stimulation of gene induction and cell growth by the Ras effector Rlf. EMBO J. *16*, 6748–6761.
38. Murai, H., et al., and Kikuchi, A. (1997). Characterization of RalGDP dissociation stimulator-like (RGL) activities to regulate c-Fos promoter and the GDP/GTP exchange of Ral. J. Biol. Chem. *272*, 10483–10490.
39. Ohnishi, M., Yamawakikataoka, Y., Kariya, K., Tamada, M., Hu, C.D., and Kataoka, T. (1998). Selective inhibition of Ras interaction with its particular effector by synthetic peptides corresponding to the Ras effector region. J. Biol. Chem. *273*, 10210–10215.
40. Polakis, P., and McCormick, F. (1993). Structural requirements for the interaction of $p21^{ras}$ with GAP, exchange factors, and its biological effector target. J. Biol. Chem. *268*, 9157–9160.
41. Wittinghofer, A., and Nassar, N. (1996). How Ras-related proteins talk to their effectors. Trends Biochem. Sci. *21*, 488–491.
42. Spoerner, M., Herrmann, C., Vetter, I.R., Kalbitzer, H.R., and Wittinghofer, A. (2001). Dynamic properties of the Ras switch I region and its importance for binding to effectors. Proc. Natl. Acad. Sci. USA. *98*, 4944–4949.
43. Fabian, J.R., Vojtek, A.B., Cooper, J.A., and Morrison, D.K. (1994). A single amino acid change in Raf-1 inhibits Ras binding and alters Raf-1 function. Proc. Natl. Acad. Sci. USA. *91*, 5982–5986.
44. Ponting, C.P., and Benjamin, D.R. (1996). A novel family of ras-binding domains. Trends Biochem. Sci. *21*, 422–425.
45. Kalhammer, G., Bahler, M., Schmitz, F., Jockel, J., and Block, C. (1997). Ras-binding domains—predicting function versus folding. FEBS Lett. *414*, 599–602.
46. Orengo, C.A., Jones, D.T., and Thornton, J.M. (1994). Protein superfamilies and domain superfolds. Nature *372*, 631–634.
47. Symons, M., et al., and Abo, A. (1996). Wiskott-Aldrich syndrome protein, a novel effector for the gtpase cdc42hs, is implicated in actin polymerization. Cell *84*, 723–734.
48. Aspenstrom, P., Lindberg, U., and Hall, A. (1996). Two GTPases, Cdc42 and Rac, bind directly to a protein implicated in the immunodeficiency disorder Wiskott-Aldrich syndrome. Curr. Biol. *6*, 70–75.
49. Rudolph, M.G., Bayer, P., Abo, A., Kuhlmann, J., Vetter, I.R., and Wittinghofer, A. (1998). The Cdc42/Rac interactive binding region motif of the Wiskott Aldrich syndrome protein (WASP) is necessary but not sufficient for tight binding to Cdc42 and structure formation. J. Biol. Chem. *273*, 18067–18076.
50. Mott, H.R., et al., and Laue, E.D. (1999). Structure of the small G protein Cdc42 bound to the GTPase-binding domain of ACK. Nature *399*, 384–388.
51. Gizachew, D., Guo, W., Chohan, K.K., Sutcliffe, M.J., and Oswald, R.E. (2000). Structure of the complex of Cdc42Hs with a peptide derived from P-21 activated kinase. Biochemistry *39*, 3963–3971.
52. Abdul-Manan, N., et al., and Rosen, M.K. (1999). Structure of Cdc42 in complex with the GTPase-binding domain of the 'Wiskott-Aldrich syndrome' protein. Nature *399*, 379–383.
53. Kim, A.S., Kakalis, L.T., Abdul-Manan, M., Liu, G.A., and Rosen, M.K. (2000). Autoinhibition and activation mechanisms of the Wiskott-Aldrich syndrome protein. Nature *404*, 151–158.
54. Manser, E., et al., and Lim, L. (1995). Molecular-cloning of a new member of the p21-cdc42/rac-activated kinase (pak) family. J. Biol. Chem. *270*, 25070–25078.
55. Martin, G.A., Bollag, G., McCormick, F., and Abo, A. (1995). A novel serine kinase activated by rac1/CDC42Hs-dependent autophosphorylation is related to PAK65 and STE20. EMBO J. *14*, 1970–1978.
56. Amano, M., et al., and Kaibuchi, K. (1997). Formation of actin stress fibers and focal adhesions enhanced by rho-kinase. Science *275*, 1308–1311.
57. Amano, M., Chihara, K., Nakamura, N., Kaneko, T., Matsuura, Y., and Kaibuchi, K. (1999). The COOH terminus of Rho-kinase negatively regulates Rho-kinase activity. J. Biol. Chem. *274*, 32418–32424.

58. Yamamori, B., Kuroda, S., Shimizu, K., Fukui, K., Ohtsuka, T., and Takai, Y. (1995). Purification of a ras-dependent mitogen-activated protein-kinase kinase kinase from bovine brain cytosol and its identification as a complex of b-raf and 14-13-3-proteins. J. Biol. Chem. *270*, 11723–11726.
59. Stokoe, D., and McCormick, F. (1997). Activation of c-Raf-1 by Ras and SRC through different mechanisms—activation in vivo and in vitro. EMBO J. *16*, 2384–2396.
60. Tu, H., and Wigler, M. (1999). Genetic evidence for Pak1 autoinhibition and its release by Cdc42. Mol. Cell. Biol. *19*, 602–611.
61. Zenke, F.T., King, C.C., Bohl, B.P., and Bokoch, G.M. (1999). Identification of a central phosphorylation site in p21-activated kinase regulating autoinhibition and kinase activity. J. Biol. Chem. *274*, 32565–32573.
62. Lei, M., et al., and Harrison, S.C. (2000). Structure of PAK1 in an autoinhibited conformation reveals a multistage activation switch. Cell *102*, 387–397.
63. Morreale, A., et al., and Laue, E.D. (2000). Structure of Cdc42 bound to the GTPase binding domain of PAK. Nat. Struct. Biol. *7*, 384–388.
64. Morrison, D.K., and Cutler, R.E. (1997). The complexity of raf-1 regulation. Curr. Opin. Cell Biol. *9*, 174–179.
65. Drugan, J.K., et al., and Campbell, S.L. (1996). Ras interaction with two distinct binding domains in raf-1 may be required for ras transformation. J. Biol. Chem. *271*, 233–237.
66. Hu, C.D., et al., and Kataoka, T. (1995). Cysteine-rich region of raf-1 interacts with activator domain of posttranslationally modified ha-ras. J. Biol. Chem. *270*, 30274–30277.
67. Lenzen, C., Cool, R.H., and Wittinghofer, A. (1995). Analysis of intrinsic and CDC25-stimulated guanine nucleotide exchange of p21ras-nucleotide complexes by fluorescence measurements. Methods Enzymol. *255*, 95–109.
68. Kabsch, W. (1993). Automatic processing of rotation diffraction data from crystals of initially unknown symmetry and cell constants. J. Appl. Crystallogr. *26*, 795–800.
69. Navaza, J. (1994). AmoRe: an automated package for molecular replacement. Acta Crystallogr. A *50*, 157–163.
70. Jones, T.A., and Kjeldgaard, M. (1997). Electron-density map interpretation. Methods Enzymol. *277*, 173–208.
71. Brünger, A.T., et al., and Warren, G.L. (1998). Crystallography & NMR system: a new software suite for macromolecular structure determination. Acta Crystallogr. D *54*, 905–921.
72. Russell, R.B., and Barton, G.J. (1992). Multiple protein sequence alignment from tertiary structure comparison: assignment of global and residue confidence levels. Proteins *14*, 309–323.
73. Kabsch, W., and Sander, C. (1983). Dictionary of protein secondary structure: pattern recognition of hydrogen-bonded and geometrical features. Biopolymers *22*, 2577–2637.
74. Gronwald, W., et al., and Hans Robert Kalbitzer. (2001). Solution structure of the Ras binding domain of the protein kinase Byr2 from *Schizosaccharomyces pombe*. Structure *9*, 1029–1041.
75.–Kraulis, P.J. (1991). MOLSCRIPT: a program to produce both detailed and schematic plots of protein structures. J. Appl. Crystallogr. *24*, 946–950.
76. Merrit, E.A. and Bacon, D.J. (1997). Raster 3D: photorealistic molecular graphics. In Methods in Enzymology, Volume 277, C.W. Carter, Jr. and R.M. Sweet, eds. (New York: Academic Press), pp. 505–524.
77. CCP4 (Collaborative Computational Project 4) (1994). The CCP4 suite: programs for protein crystallography. Acta Crystallogr. D. *50*, 760–763.

Accession Numbers

Coordinates of the Ras-Bry2RBD complex have been deposited with the Protein Data Bank under the ID code 1K8R.